





Elastic ribbons in bubble columns: When elasticity, capillarity, and gravity govern equilibrium configurations

Jean Farago , Manon Jouanlanne , Antoine Egelé , and Aurélie Hourlier-Fargette 
Université de Strasbourg, CNRS, Institut Charles Sadron UPR22, F-67000 Strasbourg, France



(Received 10 April 2024; accepted 12 July 2024; published 28 August 2024)

Taking advantage of the competition between elasticity and capillarity has proven to be an efficient way to design structures by folding, bending, or assembling elastic objects in contact with liquid interfaces. Elastocapillary effects often occur at scales where gravity does not play an important role, such as in microfabrication processes. However, the influence of gravity can become significant at the desktop scale, which is relevant for numerous situations including model experiments used to provide a fundamental physics understanding, working at easily accessible scales. We focus here on the case of elastic ribbons placed in two-dimensional bubble columns: by introducing an elastic ribbon inside the central soap films of a staircase bubble structure in a square cross-section column, the deviation from Plateau's laws (capillarity-dominated case dictating the shape of usual foams) can be quantified as a function of the rigidity of the ribbon. For long ribbons, gravity cannot be neglected. We provide a detailed theoretical analysis of the ribbon profile, taking into account capillarity, elasticity, and gravity. We compute the total energy of the system and perform energy minimization under constraints, using Lagrangian mechanics. The model is then validated via a comparison with experiments with three different ribbon thicknesses.

DOI: [10.1103/PhysRevE.110.024803](https://doi.org/10.1103/PhysRevE.110.024803)

I. INTRODUCTION

Systems involving both elastic and capillary forces have been attracting a growing interest to tackle practical challenges and provide novel engineering and design tools, compelling for the microfabrication of two-dimensional (2D) surfaces and three-dimensional (3D) structures [1,2], for the design of actuators in the emerging soft robotics field [3], but also in the context of biomechanics or biomimetic approaches [4–6], to cite only a few cases. The field of elastocapillarity includes not only the deformation of soft solids by surface tension [7], but also systems where the geometry of the elastic objects is of particular importance, especially in the context of slender structures for which bending dominates over stretching [8]. In appropriate conditions, capillary forces are sufficient to force such slender structures to undergo large deformations, in systems at multiple length scales, provided that capillary and elastic energies are of the same order of magnitude [9,10]. A fundamental understanding of elastocapillary phenomena can be acquired with experiments at the desktop scale [11,12], for systems conceptually very close to those occurring in microfabrication processes [13,14]. However, when reaching centimetric scales, the effects of gravity on slender elastic structures can be significant. Taking capillarity aside, a typical daily life experience of slender structures for which gravity matters is the shape of curly hair [15]. A few examples involving elasticity, capillarity, and gravity have been studied in the literature, for instance, in the context of floating thin elastic films [16], capillary in-drop spooling [17], elastocapillary-driven snap-through [18], and capillary rise between elastic sheets, revisiting Jurin's law in the context of elastocapillarity [19].

Here we focus on the question of the influence of gravity on the equilibrium shape of centimetric ribbons inserted inside two-dimensional bubble columns. When confined inside square cross-section tubes, bubbles rearrange themselves into well-ordered structures that depend on the confinement ratio (bubble size divided by the width of the tube) [20,21]. By choosing an appropriate ratio, we can obtain the so-called staircase structure, which is quasi-2D [Fig. 1(a)]. A ribbon can then be inserted inside the central soap films, and its shape depends on the minimization of the total energy of the system. In our previous work [22,23], we placed ourselves in conditions where gravity is negligible, by considering only the very bottom of the elastic ribbons. The total energy of the system was thus composed of the bending energy of the ribbon and of the interfacial energies, and we studied how the presence of the ribbon modified the classical Plateau's laws [24] for foams. Now, we consider long ribbons for which a flattening due to gravity is observed, especially in the upper parts, due to the weight of the lower parts.

II. MODEL DESCRIPTION AND NOTATIONS

As shown in Fig. 1, we describe a system similar to that studied in [22]. An elastic ribbon of length L is inserted in the middle of a 2D staircase arrangement of bubbles of longitudinal size 2ℓ . We divide the ribbon in half-cells (HCs), with numbers defined by starting from the bottom of the ribbon (HC no. 1 corresponds to the first half period containing a ribbon in the whole central Plateau border). The ribbon is characterized by a bending modulus per transverse length $\alpha = Et^3/[12(1 - \nu^2)]$, where t is the ribbon thickness, and (E, ν) , respectively, are the Young modulus and the Poisson

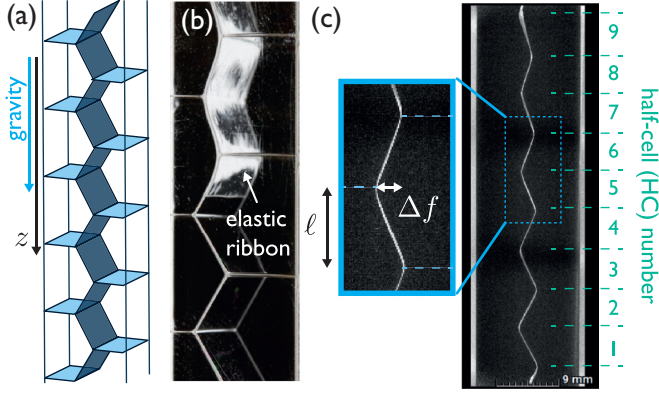


FIG. 1. Illustration of the studied system. (a) Schematic representation of a bubble column in a tube of square cross section. The ratio of the bubble size to the container dimension is chosen to obtain the so-called staircase structure [20,21], invariant by translation along the axis perpendicular to the tube. (b) Experimental visualization of the insertion of an elastic ribbon [polydimethylsiloxane (PDMS)] in a staircase bubble structure. (c) X-ray microtomography slice of the bubble column containing a thin PDMS ribbon (thickness $t = 45 \mu\text{m}$), and zoom on a half-cell presenting the definitions of the half bubble size ℓ and of the amplitude Δf . Note that the half-cell numbers are defined by starting from the bottom of the ribbon, and that the upper extremity of the ribbon is clamped above the visible part.

ratio of the ribbon, and a lineic mass per transverse length λ ($\lambda = \rho t$, with ρ the ribbon mass density). Contrary to the case studied in [22], the gravity g operating in the longitudinal Oz direction is not supposed to be negligible. Its main effect is to flatten the upper regions of the ribbon due to the weight of the lower regions pulling downwards. The purpose of the present theory is to compute the equilibrium shape of a long ribbon, tied at its upper end at $z = 0$, in the limit of a long ribbon $L/\ell \gg 1$ (to avoid finite size effects that are difficult to handle, which moreover would obscure the understanding of the theory).

The elastocapillary energy excess ΔE per unit (transverse) length of the system, with respect to the situation where only the bubbles are present, is given by

$$\Delta E = \frac{\alpha}{2} \int_0^L ds C^2 - \lambda g \int_0^L ds z(s) + 2\gamma L - \gamma \sum_{\text{HC}} [\Delta f_i + \sqrt{3}\ell], \quad (1)$$

where s is the curvilinear coordinate along the ribbon, starting from $s = 0$ at $z = 0$, $C = f''(z)/\sqrt{1 + [f'(z)]^2}$ is the local ribbon curvature [we denote $y = f(z)$ as the profile of the ribbon in the lateral direction], and Δf_i is the lateral amplitude of the ribbon deformation in the i th HC [we choose to number the HC from the bottom ($n = 1$) upward, until $n = N$]. The first three terms of the right-hand side (rhs) relate to the ribbon as, respectively, its bending, gravitational, and interfacial energies, with the latter constant term assuming a perfect wetting of the ribbon. The second line of (1) is the excess interfacial energy that the system has to pay to substitute in each HC the original liquid staircase pattern by

a wet ribbon: if h is the width of the lateral dimension of the tube [i.e., visible in Fig. 1(c)], this energy difference in the i th HC is indeed $\gamma[2L + h - \Delta f_i - (\frac{4\ell}{\sqrt{3}} + h - \frac{\ell}{\sqrt{3}})] = 2\gamma L - \gamma[\Delta f_i + \sqrt{3}\ell]$. The $\sqrt{3}\ell$ term must not be discarded as a constant due to the fact that the number of HC is variable in the optimization process.

In writing (1), one assumed that the HC size ℓ is a constant along the tube and, moreover, is unaffected by the presence of the ribbon. This approximation is justified in the Appendix. The direct minimization of (1) is complicated because the gravitational term breaks the vertical translational invariance. However, the weight of the ribbon contained in just one HC is very modest and it is relevant to assume that the gravitational energy may be considered as constant at the scale of the HC. This assumption assumes that the weight (per unit transverse length) of just one HC, $\sim \lambda g \ell$, is relatively small with respect to the typical forces (per unit transverse length), which can be either γ or α/ℓ^2 according to the considered regime (discussed below). This assumption amounts to replace $-\lambda g \int_{\text{HC}_n} ds z(s)$ by $-\lambda g(N - n + \frac{1}{2})\ell \int_{\text{HC}_n} ds$, where the integral encompasses the part of the ribbon present in the n th HC. In doing so, one assumes that the center of mass of the ribbon always stays in the middle of the HC, which is in particular provided by configurations where the ribbon shape is centrosymmetric within each HC. This would be exactly the case for the optimal ribbon shape in the n th HC if its weight was negligible because, in this case, the gravitational pulling forces exerted by the neighboring HCs on each end of the ribbon part contained in the HC would be strictly identical.

For a long ribbon, a large upper amount is totally flattened by the weight of its lower part, so it is relevant to remove from ΔE the constant energy of a totally flattened ribbon, $(\Delta E)_{\text{flat}} = 2\gamma L + \sum_{n=1}^{L/\ell} [-\lambda g(\frac{L}{\ell} - n + \frac{1}{2})\ell^2 - \gamma\sqrt{3}\ell]$, and define

$$\Delta \mathcal{E} = \Delta E - (\Delta E)_{\text{flat}} + \gamma \Lambda \left[\int ds - L \right], \quad (2)$$

where Λ is a dimensionless Lagrangian multiplier added to encode the constraint that the total length of the ribbon is conserved. If N denotes the total number of HCs that the ribbons spans, the preceding expression can be recast into

$$\Delta \mathcal{E} = \sum_{n=1}^N \left[\frac{\alpha}{2} \int_{\text{HC}_n} ds C^2 - \gamma \Delta f_n + \left[\lambda g \ell \left(n - \frac{1}{2} \right) + \gamma \Lambda \right] \left(\int_{\text{HC}_n} ds - \ell \right) \right] + \gamma \ell \mathcal{R}_N, \quad (3)$$

$$\mathcal{R}_N = \frac{\lambda g \ell}{2\gamma} (L/\ell - N)^2 + (\sqrt{3} - \Lambda)(L/\ell - N). \quad (4)$$

With this writing, one can expect that the bracketed series will be convergent if $N \rightarrow \infty$, since the large values of n will be canceled by the terms $\propto (\int ds - \ell)$, which are very small at the top of the ribbon (we will see that a remaining logarithmic divergence remains, however negligible in the limit $N \gg 1$). For the sake of simplicity, the $L/\ell \rightarrow \infty$ (which entails $N \rightarrow \infty$) limit will be systematically considered in the following. It corresponds to taking the asymptotic sum of the series in (3), but keeping in mind that $L/\ell - N$ remains finite. If finite N

corrections would have to be considered, then the boundary effects associated to the extremities of the ribbon ending, in general, in the middle of a HC should be carefully estimated, a more detailed analysis which is beyond the scope of this work.

We make the problem dimensionless by defining

$$\widehat{\lambda} = \frac{\lambda g \ell}{\gamma}, \quad (5)$$

$$\eta = \frac{\alpha}{\gamma \ell^2}, \quad (6)$$

and writing (note that $\Delta \mathcal{E}$ is an energy per transverse unit length)

$$\Delta \mathcal{E}/[\gamma \ell] = \sum_{n=1}^N e_n + \mathcal{R}_N, \quad (7)$$

$$e_n = \frac{\eta}{2} \int_{\text{HC}_n} \frac{ds}{\ell} (C\ell)^2 + \eta \kappa_n^2 \left(\int_{\text{HC}_n} \frac{ds}{\ell} - 1 \right) - \frac{\Delta f_n}{\ell}, \quad (8)$$

$$\kappa_n^2 = \frac{\widehat{\lambda} \left(n - \frac{1}{2} \right) + \Lambda}{\eta}. \quad (9)$$

In the preceding formula, the curvature C is related to the profile $f(z)$ of the ribbon by the already mentioned classical formula $C = f''(z)/\sqrt{1 + [f'(z)]^2}$, and $ds = \sqrt{df^2 + dz^2} = dz\sqrt{1 + [f'(z)]^2}$. The optimization of (7) consists in (i) writing the Euler-Lagrange equations for $f(z)$ of the ribbon in each HC separately, which is possible since the optimal solution has extrema at the boundaries of the HC; (ii) expressing the constraint “ribbon length = L ” to remove N from (7) in favor of Λ ; and (iii) extremalizing the resulting expression for $\Delta \mathcal{E}$ with respect to Λ , which is equivalent to (but easier than) extremalizing with respect to N . Notice that the whole optimal solution is twice differentiable everywhere with slight discontinuities of the second derivatives at the boundaries of HC, which is not forbidden by the physics, as the lateral liquid interfaces act as localized (“impulsive”) normal forces at these boundaries on the ribbon.

In the general case, the optimization of (7) is probably intractable, but as in [22], we can separately solve the case $\eta \gg 1$ (stiff ribbons), where the ribbon remains everywhere almost flat, and $\eta \ll 1$ (soft ribbons), where the ribbon only slightly perturbs the Plateau’s laws. In the latter case, a slight difficulty must be overcome since the gravity significantly flattens the bubbles in the upper parts of a long enough ribbon, even if the ribbon elasticity does not.

A. Stiff ribbon limit: $\eta \gg 1$

This case is certainly less relevant experimentally, but it is theoretically instructive, because much simpler to proceed with. Here, $f \ll \ell$ everywhere and it is relevant to Taylor-expand e_n up to the second order,

$$e_n \simeq \frac{\eta \ell}{2} \int_0^\ell dz [f''(z)]^2 + \frac{\eta \kappa_n^2 \ell^{-1}}{2} \int_0^\ell dz [f'(z)]^2 - \frac{\Delta f_n}{\ell} \quad (10)$$

(notice that a translation in z is made so that z spans the interval $[0, \ell]$ whatever the HC that is considered). One writes $f(z) = (\Delta f_n) g_n(z/\ell)$ since the particular structure of (10) allows a separate optimization of the shape $g_n(z/\ell)$ and

the amplitude Δf_n of the profile. Solving the fourth-order Euler-Lagrange equation with the four boundary conditions $[g_n(0) = 0, g_n(1) = 1, g'_n(0) = g'_n(1) = 0]$ gives, for the optimal shape [25],

$$g_{n,\text{opt}} \left(u = \frac{z}{\ell} \right) = \frac{\tanh\left(\frac{\kappa_n}{2}\right) [\cosh(\kappa_n u) - 1] + \kappa_n u - \sinh(\kappa_n u)}{\kappa_n - 2 \tanh\left(\frac{\kappa_n}{2}\right)}. \quad (11)$$

To get the optimal value of Δf_n , we express the energy e_n optimized with respect to g_n as

$$e_n = \frac{\eta}{2} \left(\frac{\Delta f_n}{\ell} \right)^2 \int_0^1 du g'_{n,\text{opt}} \left[-g_{n,\text{opt}}^{(3)} + \kappa_n^2 g'_{n,\text{opt}} \right] - \frac{\Delta f_n}{\ell}. \quad (12)$$

By optimizing e_n with respect to Δf_n , we obtain

$$\frac{\Delta f_{n,\text{opt}}}{\ell} = \eta^{-1} \frac{\kappa_n - 2 \tanh\left(\frac{\kappa_n}{2}\right)}{\kappa_n^3}, \quad (13)$$

$$e_{n,\text{opt}} = -\frac{1}{2} \frac{\Delta f_{n,\text{opt}}}{\ell}. \quad (14)$$

As announced in anticipation, it can be observed that the optimal value of the series in (7) keeps a slight divergence since $e_{n,\text{opt}} \sim -\frac{1}{2\lambda n}$ for large values of n . This divergence gives a term $\propto \ln(N)$, which we make explicit by writing

$$\sum_{n=1}^N e_{n,\text{opt}} \simeq \sum_{n=1}^{\infty} \left[e_{n,\text{opt}} + \frac{1}{2\lambda n} \right] - \frac{\ln N}{2\lambda}. \quad (15)$$

The constraint that the ribbon length in the optimal shape is L reads $L/\ell - N_{\text{opt}} = \ell^{-1} \sum_{\text{HC}} [f ds - \ell]$, and up to the second order in f_n ,

$$L/\ell - N = \frac{1}{2} \sum_{n=1}^{N_{\text{opt}}} \left(\frac{\Delta f_n}{\ell} \right)^2 \int_0^1 du g'_{n,\text{opt}}(u)^2 \sim \mathcal{S}, \quad (16)$$

$$\mathcal{S} = \frac{1}{2\eta^2} \sum_{n=1}^{\infty} \frac{1}{\kappa_n^5} \left[-\frac{\kappa_n}{2} \tanh^2\left(\frac{\kappa_n}{2}\right) + 3\frac{\kappa_n}{2} - 3 \tanh\left(\frac{\kappa_n}{2}\right) \right], \quad (17)$$

where the summation has been pushed to $+\infty$ since the series is convergent. Note that $\mathcal{S} = \partial_\Lambda \sum [e_{n,\text{opt}} + 1/(2\lambda n)]$, which is understood by considering Eq. (10): The derivative of this expression with respect to Λ has two parts, one implicit because f depends on Λ , which is identically zero because a first-order variation of the optimal f is always zero whatever its value, and one explicit because κ_n^2 depends on Λ , which gives exactly the second-order approximation to $L/\ell - N$, i.e., \mathcal{S} . Note, also, that we discarded the term $\propto \ln(N)$ which induces negligible corrections for long enough ribbons. Finally, one uses (4), (7), and (16) to write

$$\Delta \mathcal{E}/\gamma \ell = \sum_{n=1}^{\infty} \left[e_{n,\text{opt}} + \frac{1}{2\lambda n} \right] + \frac{\widehat{\lambda}}{2} \mathcal{S}^2 + (\sqrt{3} - \Lambda) \mathcal{S}. \quad (18)$$

This expression has to be optimized with respect to Λ , a step equivalent to finding the optimal number N_{opt} of HC spanned by the ribbon at equilibrium [via Eq. (16)]. The fact that $\partial_\Lambda \sum [e_{n,\text{opt}} + 1/(2\lambda n)] = \mathcal{S}$ shows that the equation fulfilled by the optimal Λ is either $\partial_\Lambda \mathcal{S} = 0$ (which is impossible

because $e_{n,\text{opt}}$ is a convex function of Λ) or

$$\frac{\Lambda - \sqrt{3}}{\widehat{\lambda}} = S. \quad (19)$$

To go further, one can evaluate numerically the preceding expression and solve for Λ , but one can also make use of the fact that $\eta \gg 1$. For small values of $\widehat{\lambda}/\eta = \lambda g \ell^3/\alpha$, the parameter κ_n is slowly varying with n , and we can use the Euler-MacLaurin formula and replace the sum in (17) with an integral (plus the correction terms “ $\frac{f(1)}{2} - \frac{f'(1)}{12}$ ” [26] to be comprehensive at the order η^{-4}). After a cumbersome calculation, one finds

$$\Lambda = \sqrt{3} + \frac{1}{24\eta} - \frac{\sqrt{3}}{240\eta^2} + \frac{11 - \frac{17}{48}\widehat{\lambda}^2}{10080\eta^3} + o(\eta^{-3}). \quad (20)$$

It is remarkable that the first three orders of the expansion do not depend on $\widehat{\lambda}$. This expression corresponds to the limit of large η at constant $\widehat{\lambda}$, and can also be used in the experimentally relevant limit of large t , with $\eta \propto t^3$ and $\widehat{\lambda} \propto t$. The term $\propto \widehat{\lambda}^2 \eta^{-3}$ must in this case be considered as $O(t^{-7})$ and overcomes the $O(\eta^{-3}) = O(t^{-9})$ one.

Another interesting case corresponds to $\widehat{\lambda} = 0$ whatever η . In this case, the lowest approximation for κ_n in the case $\widehat{\lambda} = 0$ is $\kappa_n \sim 3^{1/4}/\sqrt{\eta}$, a result we obtained in [22] (formula (11) in [22], $\kappa_n \equiv 2\kappa$). The shape g_n and the transverse amplitude Δf_n are also the same).

Particularly interesting is the evolution of $\Delta f_n/\ell$ with $n = O(1)$ (lower part of the ribbon). In the approximation $\eta \gg 1$ that we are considering here, κ_n is, for the lower part of the ribbon, a small quantity and one can approximate (13) by

$$\frac{\sqrt{3}\Delta f_{n,\text{opt}}}{\ell} = \frac{1}{4\sqrt{3}\eta} \left[1 - \frac{\sqrt{3} + \widehat{\lambda}(n - \frac{1}{2})}{10\eta} \right]. \quad (21)$$

As a result, a linear reduction of the lateral amplitude can be expected, with a slope $\widehat{\lambda}/[40\sqrt{3}\eta^2]$ quite small with reasonable values of $\widehat{\lambda}$ and $\eta \gg 1$. This limit, $\eta \gg 1$, therefore does not appear as a relevant one to capture a signature of the gravitational effects. However, the theory is particularly clear. In the next paragraph, the same line of reasoning is followed in the opposite limit, when $\eta \ll 1$, which is a more complicated case due essentially to the fact that it is an expansion around a singular solution, reminiscent, for instance, of the zero-temperature expansion of fermionic gas.

B. Floppy ribbon limit: $\eta \ll 1$

1. The $\eta = 0$ case

In this opposite limit, the gravitational pull and the elastocapillary interaction oppose each other since the capillarity largely dominates the forces opposing the bending and forces the ribbon to a winding shape. To tackle this case, it is useful to note that $\widehat{\lambda} \propto t$ (t is the ribbon thickness), whereas $\eta \propto t^3$, which suggests that one first considers the case where formally $\eta = 0$ and $\widehat{\lambda} \neq 0$. We define

$$\omega_n^2 = \widehat{\lambda} \left(n - \frac{1}{2} \right) + \Lambda, \quad (22)$$

instead of $\kappa_n^2 = \omega_n^2/\eta$. The energy terms now read

$$e_n^\circ = \omega_n^2 \int_0^\ell \frac{dz}{\ell} \{ \sqrt{1 + [f'(z)]^2} - 1 \} - \frac{\Delta f_n}{\ell}. \quad (23)$$

The optimal shape is readily $g^\circ(u) = u$, from which we deduce the optimal amplitude Δf_n° ,

$$\omega_n^2 \frac{\Delta f_n^\circ/\ell}{\sqrt{1 + (\Delta f_n^\circ/\ell)^2}} - 1 = 0 \Rightarrow \frac{\Delta f_n^\circ}{\ell} = \frac{1}{\sqrt{\omega_n^4 - 1}}, \quad (24)$$

and the optimal energy $e_n^\circ = \sqrt{\omega_n^4 - 1} - \omega_n^2$. Once again, the series in (7) has a logarithmic divergence, and we write, in the large L/ℓ limit,

$$\Delta \mathcal{E}^\circ/[\gamma \ell] \simeq \sum_{n=1}^{\infty} \left[e_n^\circ + \frac{1}{2\widehat{\lambda}n} \right] - \frac{1}{2\widehat{\lambda}} \ln(N) + \mathcal{R}_N. \quad (25)$$

One finds the same type of calculations as before, and the ribbon length constraint equation (16) is written as

$$\frac{\Lambda - \sqrt{3}}{\widehat{\lambda}} = \sum_{n=1}^{\infty} \frac{\omega_n^2 - \sqrt{\omega_n^4 - 1}}{\sqrt{\omega_n^4 - 1}}, \quad (26)$$

where the series in the rhs is convergent. This equation is the self-consistent equation setting the value of Λ (present in the ω_n as well). It is important to note (regarding the next section) that as for the $\eta \gg 1$ case, $\partial_\Lambda (\sum_n e_n^\circ) = L/\ell - N$, which yields a similar structure between Eqs. (19) and (26).

The limit $\widehat{\lambda} \rightarrow 0$ is instructive. The right-hand side series is found (using the Euler-MacLaurin formula) equivalent to $[\Lambda - \sqrt{\Lambda^2 - 1}]/\widehat{\lambda}$, which gives $\Lambda \sim 2$ in this limit. This is coherent in (24) with the value $\Delta f_n^\circ/\ell = 1/\sqrt{3}$ expected everywhere in this limit $\widehat{\lambda} = \eta = 0$.

2. $\eta \ll 1$ is a singular expansion

To account for the cases where $\eta \ll 1$, but nonzero, the idea is to expand from the preceding solution. A key point is that the preceding solution is piecewise linear and therefore not twice differentiable as expected for a ribbon with a finite bending modulus. As a result, a naive expansion is bound to fail since the perturbative term should “cure” the zeroth-order singularity to yield a regular solution, which is just impossible.

To tackle this difficulty, one formally writes $f_n(z) = \frac{\Delta f_n^\circ}{\ell} z + \xi_n(z)$, where ξ_n is a small departure from a zeroth order, which is similar to that computed in Sec. II B 1, but for the value Λ , which is not fixed at the zeroth order by (26), but will be later on. One makes a Taylor expansion of the energy up to the second order in (8) and (9), which gives

$$e_n = e_n^\circ + \frac{\eta \ell}{2} \frac{\omega_n^2 (\omega_n^4 - 1)^{1/4}}{(\omega_n^4 - 1)^{3/4} + 1} \left\{ \int_0^\ell dz [(\xi_n'')^2 + k_n^2 (\ell^{-1} \xi_n')^2] \right\}, \quad (27)$$

where

$$k_n^2 = \frac{1}{\eta} \frac{(\omega_n^4 - 1)^{5/4} [(\omega_n^4 - 1)^{3/4} + 1]}{\omega_n^6}, \quad (28)$$

and wherein ω_n^2 the value of Λ is yet to be determined.

At this point, it is crucial to express (27) back in terms of f_n and optimize the energy with respect to f_n rather than ξ_n (a path also followed in [22]). The reason is that the expected solution is at least C^1 and even twice differentiable, and that the zeroth order of our expansion is singular with respect to this requirement. As a result, as we cannot expect to recover with $\frac{\Delta f_n^\circ}{\ell} z + \xi_n(z)$ a twice differentiable solution, since $\xi_n(z)$ would be twice differentiable as the result of an optimization process, it is compulsory to reexpress ξ_n in (27) in terms of f_n and do the optimization directly on f_n . It is interesting to note that no obvious alternate method seems at hand to solve this issue and produce a first-order expansion in η of the solution with the required regularity. This singularity will be manifest in the fact that the first correction to Δf_n° in Δf will be $O(\sqrt{\eta})$, not $O(\eta)$.

Owing to these remarks, one writes (27), making the substitution $\xi'_n = f'_n - \Delta f_n^\circ/\ell$ and $\xi''_n = f''_n$, to obtain

$$e_n = e_n^\circ + \frac{\eta\ell}{2} \frac{\omega_n^2(\omega_n^4 - 1)^{1/4}}{(\omega_n^4 - 1)^{3/4} + 1} \left\{ \int_0^\ell dz [(f_n'')^2 + k_n^2(\ell^{-1} f_n')^2] \right\} + \frac{1}{2\omega_n^4} \left[\sqrt{\omega_n^4 - 1} - 2(\omega_n^4 - 1) \frac{\Delta f_n}{\ell} \right]. \quad (29)$$

Comparison between (29) and (10) shows that $f_n(z) = \Delta f_n h_n(u = z/\ell)$, where h_n is given by the same formula as for g_n in (11), but with k_n replacing κ_n . Likewise, the amplitude Δf_n minimizes

$$e_{n,\text{opt}} - e_n^\circ = \frac{1}{2} \frac{k_n(\omega_n^4 - 1)^{3/2}}{\omega_n^4(k_n - 2 \tanh \frac{k_n}{2})} \left(\frac{\Delta f_n}{\ell} \right)^2 + \frac{1}{2\omega_n^4} \left[\sqrt{\omega_n^4 - 1} - 2(\omega_n^4 - 1) \frac{\Delta f_n}{\ell} \right], \quad (30)$$

from which one gets

$$\frac{\Delta f_{n,\text{opt}}}{\ell} = \left(1 - \frac{\tanh \frac{k_n}{2}}{k_n/2} \right) \left(\frac{1}{\sqrt{\omega_n^4 - 1}} \right) \quad (31)$$

and

$$e_{n,\text{opt}} = e_n^\circ + \frac{\sqrt{\omega_n^4 - 1}}{\omega_n^4 k_n} \tanh \frac{k_n}{2}, \quad (32)$$

which shows that the correction to the energy is consequently a convergent series. In (31), Λ (implicit in ω_n^2 and k_n) is given by taking into account the constraint equation expressing that the length of the ribbon is L . Up to the first order in $\xi'_n = f'_n - \Delta f_n^\circ/\ell$, this is

$$\begin{aligned} S^\dagger(\Lambda) &= \frac{L}{\ell} - N \\ &= \sum_n \left[\frac{\omega_n^2 - \sqrt{\omega_n^4 - 1}}{\sqrt{\omega_n^4 - 1}} - \frac{1 + 3\omega_n^4}{4\omega_n^6 \sqrt{\omega_n^4 - 1}} \frac{\tanh \frac{k_n}{2}}{k_n/2} \right] \\ &\quad + \sum_n \frac{\sqrt{\omega_n^4 - 1}}{4\omega_n^6} \left[1 - \tanh^2 \frac{k_n}{2} \right]. \end{aligned} \quad (33)$$

The value of Λ is finally found as the one minimizing

$$\frac{\Delta \mathcal{E}(\Lambda)}{\gamma \ell} = \sum_{n=1}^{\infty} \left[e_{n,\text{opt}} + \frac{1}{2\widehat{\lambda}n} \right] + \frac{\widehat{\lambda}}{2} S^{\dagger 2} + (\sqrt{3} - \Lambda) S^\dagger, \quad (34)$$

which is simply done using, for instance, MATLAB. It is worth noting that here the structure of the equation is more complicated than before ($\eta \gg 1$ or $\eta = 0$ cases). This is due to the fact that in (29), the explicit (i.e., not in f_n) dependence of the expression with respect to Λ is not of the form $\Lambda(L/\ell - N)$ (as before), but also involves the curvature energy term. Consequently, we no longer have $\partial_\Lambda \sum_n [e_{n,\text{opt}} + 1/(2\widehat{\lambda}n)]$ equating S^\dagger , and (34) does not boil down to $(\Lambda - \sqrt{3})/\widehat{\lambda} = S^\dagger$ anymore.

III. COMPARISON WITH EXPERIMENTS

A. Materials and methods

A bubble column is produced by bubbling air via a pressure controller through a nozzle in a detergent solution [composed of water with 4.5 vol% Fairy (dishwashing liquid, used as a surfactant), 1.5 vol% Glycerol (Sigma-Aldrich), and 10 g L⁻¹ J-Lube lubricant (Jorgensen Labs)]. Once the square cross-section tube of width 15 mm is filled with bubbles, a polydimethylsiloxane thin ribbon (PDMS Sylgard 184, Dow Corning, 10:1 base to curing agent ratio, cured at 60 °C) of width 14.5 ± 0.1 mm, hydrophilized via plasma cleaning treatment on both sides, is inserted in the central Plateau border. All details of the preparation procedure can be found in our previous article [22] and are visually highlighted in the video provided in the Supplemental Material [27]. The surface tension of the solution is $\gamma = 26 \pm 1$ mN/m, the thickness of the ribbons are varied using different spin-coating speeds ($t = 45, 55,$ and 127 μm), and the elastic material parameters are taken as $E = 1.7 \pm 0.2$ MPa for the Young's modulus, 0.45 for the Poisson's ratio, and $\rho = 1027$ kg m⁻³ for the mass density.

A specific care has been given in the current work to avoid any 3D effect in the case of long ribbons. To do so, the top of the ribbon has been pierced with six holes of 2 mm diameter, equally spaced on a horizontal line, to release lateral constraints at the upper clamping point. We also noticed that when the bottom of the ribbon arrives right at a node of the bubble column, there can be a pinning force exerted on the system, so we avoided this case and considered systems where the end of the ribbon is not at the extremity of a half-cell.

The structure is allowed to drain for 30 minutes, to avoid motion artifacts, and is then scanned with an x-ray microtomograph EasyTom 150/160 (RX Solutions). A helical scan of 48 minutes is performed at resolution 12 μm to capture the deformation of the ribbon. The 3D image is then converted into 100 slices equally spaced, taken on planes perpendicular to the ribbon. On each slice, the amplitude of the deformation Δf and the half-cell size ℓ are measured, and values are averaged over the 100 slices.

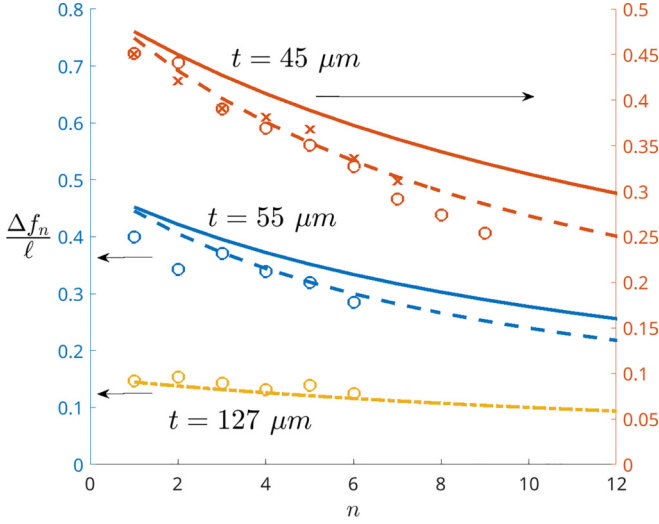


FIG. 2. Decrease of $\Delta f_n/\ell$ as a function of n for three different ribbon thicknesses : $t = 45 \mu\text{m}$ (red), $t = 55 \mu\text{m}$ (blue), and $t = 127 \mu\text{m}$ (yellow). The symbols are results of measurements from experiments (two different samples for $t = 45 \mu\text{m}$), the solid lines are the result of the theory of Sec. II B ($\eta \ll 1$) without adjustable parameters, the dashed lines are the results of the theory where the dimensionless mass density $\hat{\lambda}$ has been adjusted (with a factor 1.4 and 1.5 for the red and blue curves, respectively), and the yellow dash-dotted curve is the result of the theory of Sec. II A ($\eta \gg 1$). Notice that for the sake of readability, the red curves on the y axis are located to the right, whereas the other's is to the left. For the three experiments, the average values of ℓ are, respectively, 5.7, 6.3, and 6.0 mm and the associated η are 1.9×10^{-2} , 2.8×10^{-2} , and 0.38.

B. Results and discussion

We compared the prediction of the above theory with experiments and the results are plotted in Fig. 2, where three different ribbons with different thicknesses were tested. For the thicknesses $t = 45 \mu\text{m}$ and $t = 55 \mu\text{m}$, the parameters η are, respectively, 1.9×10^{-2} and 2.8×10^{-2} and it is relevant to use the theory of Sec. II B. Interestingly, the theory correctly predicts $\Delta f_1/\ell$, but slightly underestimates the decrease of $\Delta f_n/\ell$, which is correctly taken into account only if the dimensionless mass density $\hat{\lambda}$ is allowed to be renormalized by a factor 1.4–1.5. This discrepancy could be accounted for by the potential presence of two thin liquid layers of thickness of the order of $t_w \sim 10 \mu\text{m}$ each, coating the hydrophilic ribbon on each side. The complex rheologic nature of the liquid that is used allows long-lasting structures, but also slows down drainage, which makes this hypothesis likely. In the case of a thicker ribbon $t = 127 \mu\text{m}$, we used the theory of Sec. II A ($\eta \gg 1$), which captures well the experimental data, as shown in yellow in Fig. 2.

IV. CONCLUSION

In this work, we have tackled the question of the equilibrium shape of elastic ribbons in 2D bubble columns, in the case where gravity, capillarity, and elasticity compete to set

the equilibrium architecture. We have performed the analysis in multiple limit cases and highlighted the most relevant one (floppy ribbon limit, for which gravity, capillarity, and elasticity all significantly matter in the shape optimization). This specific problem is fundamentally interesting as it involves an optimization around a singular shape, provided by Plateau's laws when bubbles only are present. Finally, we have successfully compared our analysis to experiments with multiple ribbon thicknesses, providing evidence of the importance of considering gravity in such systems and assessing the validity of our modeling.

ACKNOWLEDGMENTS

We are grateful to W. Drenckhan, T. Charitat, and F. Schosseler for fruitful discussions, to D. Favier for his help in some preliminary tomography experiments, to the ICS PECCAT team, and especially F. Boulmedais, for the access to a spin-coater tool and a plasma cleaner, and to C. Lambour for the fabrication of the square-section tube. We also thank C. Loth and T. Schutz for their help in the recording of the Supplemental Material video [27]. This work of the Interdisciplinary Institute HiFunMat, as part of the ITI 2021-2028 program of the University of Strasbourg, CNRS and Inserm, was supported by IdEx Unistra (Grant No. ANR-10-IDEX-0002) and SFRI (STRAT'US project, Grant No. ANR-20-SFRI-0012) under the framework of the French Investments for the Future Program. We also acknowledge funding from the IdEx Unistra framework (A.H.-F.) and from the ANR (FOAMINT project, Grant No. ANR-23-CE06-0014-01).

APPENDIX: JUSTIFICATION OF THE APPROXIMATION

$\ell = \text{const}$

The volume variations induced by the ribbon are tiny and negligible, and $\ell = \text{const}$ is a good approximation, provided the experimental setup warrants the generation of identical bubbles. To see this, one balances the deformation work done on a bubble by the typical energy of curvature of a zigzagging ribbon: $\delta V/V \simeq \alpha/P_0 V$, where V is a bubble volume (the geometry of the staircase bubbles is such that all relevant typical length scales, either direct or transverse, have the same order of magnitude, ℓ). With typical values for (α, P_0, V) , one gets $\delta\ell/\ell \sim \delta V/V \sim 10^{-5}$, which validates the constant ℓ assumption. Another even more important source of volume variation is associated to the fact that the ribbon thickness is not entirely negligible with respect to the tube lateral size: for a ribbon of size $\sim 100 \mu\text{m}$, the induced (negative) volume variations are *a priori* $\delta V/V \sim 10^{-2}$. If the pressure stays constant, δV must actually vanish, which would occur via a (positive) variation $\delta\ell/\ell \sim 10^{-2}$ between a HC with a ribbon and a HC without. If the pressure actually increases slightly, $\delta\ell/\ell$ is even smaller. All in all, we remark that $\delta\ell/\ell$ is always quite small and we will henceforth neglect its variations.

- [1] M. De Volder and A. J. Hart, Engineering hierarchical nanostructures by elastocapillary self-assembly, *Angew. Chem., Intl. Ed.* **52**, 2412 (2013).
- [2] K. S. Kwok, Q. Huang, M. Mastrangeli, and D. H. Gracias, Self-folding using capillary forces, *Adv. Mater. Interfaces* **7**, 1901677 (2020).
- [3] L. Hines, K. Petersen, G. Z. Lum, and M. Sitti, Soft actuators for small-scale robotics, *Adv. Mater.* **29**, 1603483 (2017).
- [4] M. Heil, A. L. Hazel, and J. A. Smith, The mechanics of airway closure, *Respir. Physiol. Neurobiol.* **163**, 214 (2008).
- [5] S. Gernay, W. Federle, P. Lambert, and T. Gilet, Elastocapillarity in insect fibrillar adhesion, *J. R. Soc. Interface* **13**, 20160371 (2016).
- [6] H. Elettro, S. Neukirch, F. Vollrath, and A. Antkowiak, In-drop capillary spooling of spider capture thread inspires hybrid fibers with mixed solid-liquid mechanical properties, *Proc. Natl. Acad. Sci. USA* **113**, 6143 (2016).
- [7] R. W. Style, A. Jagota, C.-Y. Hui, and E. R. Dufresne, Elastocapillarity: Surface tension and the mechanics of soft solids, *Annu. Rev. Condens. Matter Phys.* **8**, 99 (2017).
- [8] D. P. Holmes, Elasticity and stability of shape-shifting structures, *Curr. Opin. Colloid Interface Sci.* **40**, 118 (2019).
- [9] B. Roman and J. Bico, Elastocapillarity: Deforming an elastic structure with a liquid droplet, *J. Phys.: Condens. Matter* **22**, 493101 (2010).
- [10] J. Bico, É. Reyssat, and B. Roman, Elastocapillarity: When surface tension deforms elastic solids, *Annu. Rev. Fluid Mech.* **50**, 629 (2018).
- [11] J. Bico, B. Roman, L. Moulin, and A. Boudaoud, Adhesion: Elastocapillary coalescence in wet hair, *Nature (London)* **432**, 690 (2004).
- [12] C. Py, P. Reverdy, L. Doppler, J. Bico, B. Roman, and C. N. Baroud, Capillary origami: Spontaneous wrapping of a droplet with an elastic sheet, *Phys. Rev. Lett.* **98**, 156103 (2007).
- [13] K. K. S. Lau, J. Bico, K. B. K. Teo, M. Chhowalla, G. A. J. Amaratunga, W. I. Milne, G. H. McKinley, and K. K. Gleason, Superhydrophobic carbon nanotube forests, *Nano Lett.* **3**, 1701 (2003).
- [14] A. Legrain, T. G. Janson, J. W. Berenschot, L. Abelmann, and N. R. Tas, Controllable elastocapillary folding of three-dimensional micro-objects by through-wafer filling, *J. Appl. Phys.* **115**, 214905 (2014).
- [15] J. T. Miller, A. Lazarus, B. Audoly, and P. M. Reis, Shapes of a suspended curly hair, *Phys. Rev. Lett.* **112**, 068103 (2014).
- [16] J. Huang, B. Davidovitch, C. D. Santangelo, T. P. Russell, and N. Menon, Smooth cascade of wrinkles at the edge of a floating elastic film, *Phys. Rev. Lett.* **105**, 038302 (2010).
- [17] H. Elettro, A. Antkowiak, and S. Neukirch, The heavy windlass: Buckling and coiling of an elastic rod inside a liquid drop in the presence of gravity, *Mech. Res. Commun.* **93**, 58 (2018).
- [18] A. Fargette, S. Neukirch, and A. Antkowiak, Elastocapillary snapping: Capillarity induces snap-through instabilities in small elastic beams, *Phys. Rev. Lett.* **112**, 137802 (2014).
- [19] H.-Y. Kim and L. Mahadevan, Capillary rise between elastic sheets, *J. Fluid Mech.* **548**, 141 (2006).
- [20] S. Hutzler, J. Barry, P. Grasland-Mongrain, D. Smyth, and D. Weaire, Ordered packings of bubbles in columns of square cross-section, *Colloids Surf., A* **344**, 37 (2009).
- [21] D. Reinelt, P. Boltenhagen, and N. Rivier, Deformed foam structure and transitions in a tube, *Eur. Phys. J. E* **4**, 299 (2001).
- [22] M. Jouanlanne, A. Egelé, D. Favier, W. Drenckhan, J. Farago, and A. Hourlier-Fargette, Elastocapillary deformation of thin elastic ribbons in 2D foam columns, *Soft Matter* **18**, 2325 (2022).
- [23] O. Shishkov, A. Blonder, S. Gowen, T. J. Jones, M. Jouanlanne, Q. Zhang, E. Del Gado, and I. Bischofberger, First annual APS DSOFT gallery of soft matter, *Phys. Rev. E* **106**, 050001 (2022).
- [24] J. A. F. Plateau, *Experimental and Theoretical Statics of Liquids Subject to Molecular Forces Only* (Gauthier-Villars, Trübner and Co., 1873).
- [25] As we consider only half-cells (HC), one should impose $g_n(0) = 1$ and $g_n(1) = 0$ every two HCs. But this point does not change any of the conclusions in the adopted assumption of light ribbons, so we impose $g(0) = 0$ and $g(1) = 1$ everywhere for the sake of simplicity.
- [26] NIST Digital Library of Mathematical Functions, edited by F. W. J. Olver, A. B. Olde Daalhuis, D. W. Lozier, B. I. Schneider, R. F. Boisvert, C. W. Clark, B. R. Miller, B. V. Saunders, H. S. Cohl, and M. A. McClain, <https://dlmf.nist.gov/>.
- [27] See Supplemental Material at <http://link.aps.org/supplemental/10.1103/PhysRevE.110.024803> for video presenting the experimental aspects, from the production of the bubble column to the introduction of the flexible ribbon in the column.